Exploring complex normal faulting systems through physics-based dynamic rupture modeling

Cycle Team Meeting

Hugo S.

Institut de Recherche pour le Dveloppement IRD - ISTerre

O., Scotti, S., Hok, A.-A. Gabriel and T. Taufiqurrahman

ANR EQTIME Project

May 12, 2022

Outline

Motivation

Preliminary exploration

Motivation

Seismic Hazard in Central Italy

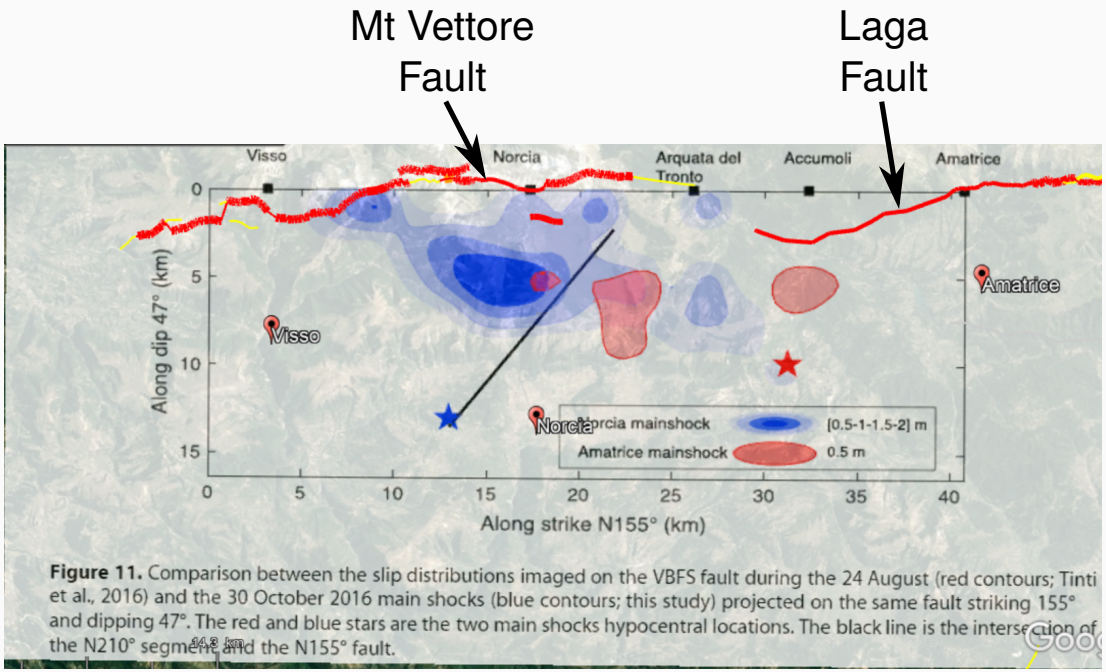

Figure 11. Comparison between the slip distributions imaged on the VBFS fault during the 24 August (red contours; Tinti et al., 2016) and the 30 October 2016 main shocks (blue contours; this study) projected on the same fault striking 155° and dipping 47°. The red and blue stars are the two main shocks hypocentral locations. The black line is the intersection of the N210° segment and the N155° fault.

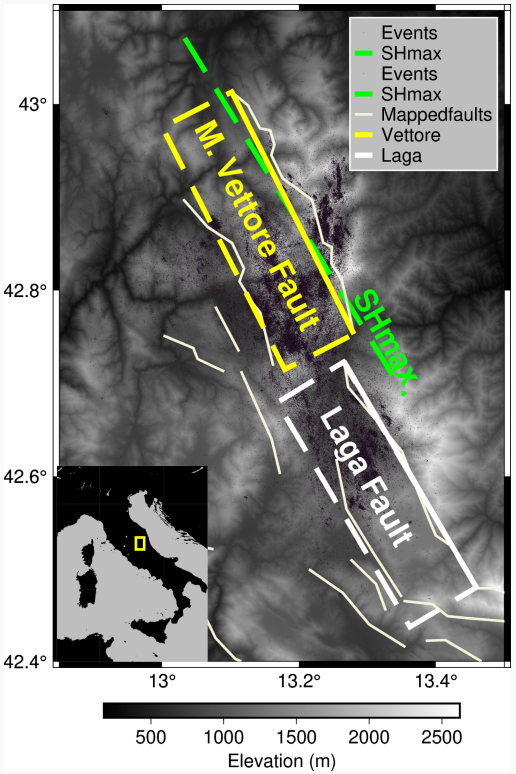

Modified by O. Scotti from Scognamiglio et al. (2018)

Seismic Hazard in Central Italy

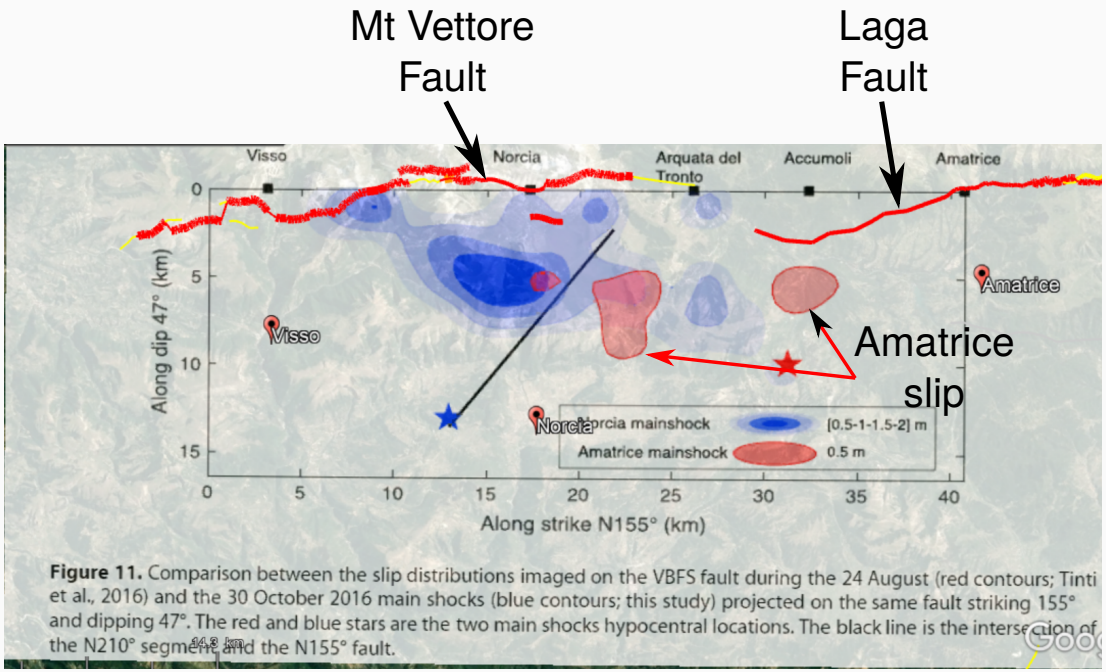

Figure 11. Comparison between the slip distributions imaged on the VBFS fault during the 24 August (red contours; Tinti et al., 2016) and the 30 October 2016 main shocks (blue contours; this study) projected on the same fault striking 155° and dipping 47°. The red and blue stars are the two main shocks hypocentral locations. The black line is the intersection of the N210° segment and the N155° fault.

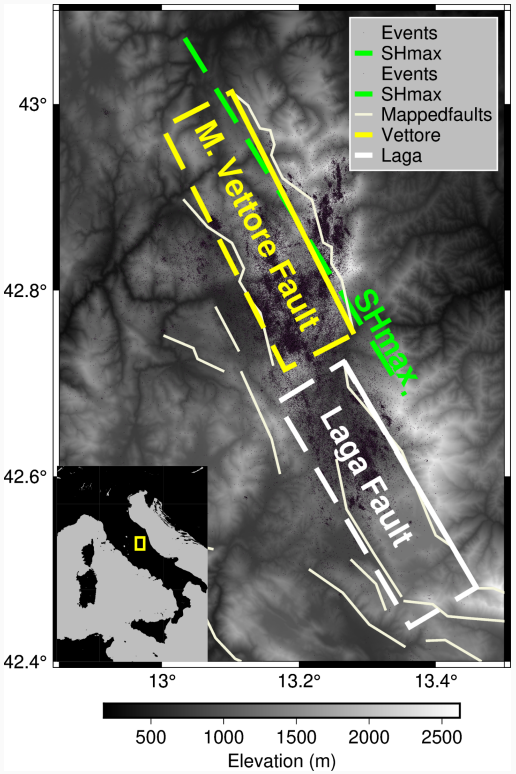

Modified by O. Scotti from Scognamiglio et al. (2018)

Seismic Hazard in Central Italy

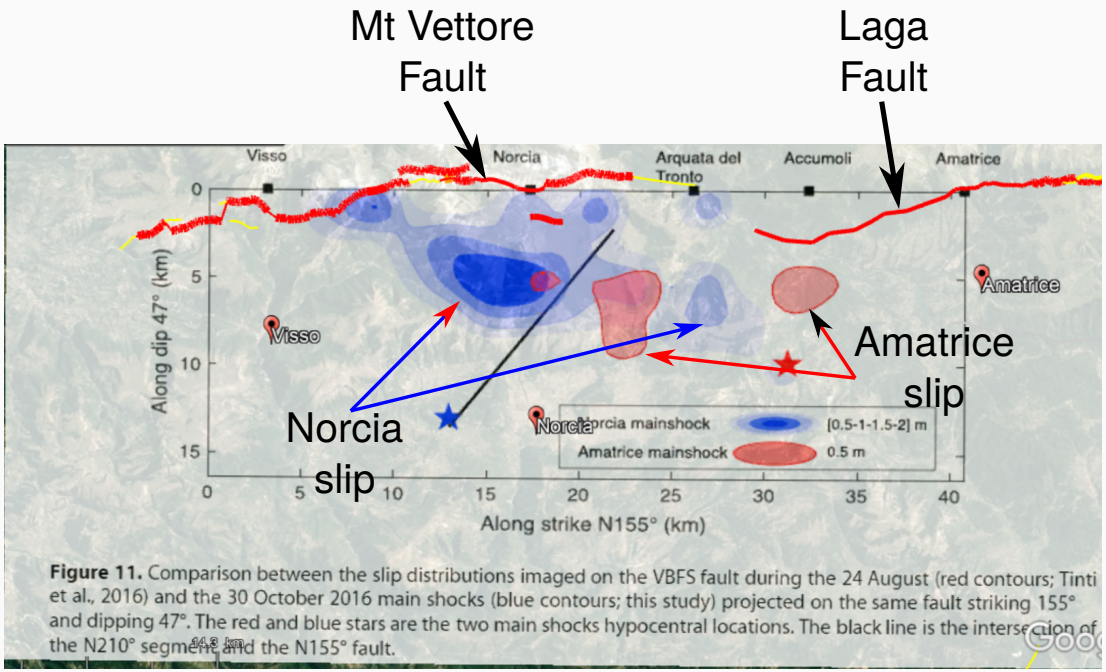

Figure 11. Comparison between the slip distributions imaged on the VBFS fault during the 24 August (red contours; Tinti et al., 2016) and the 30 October 2016 main shocks (blue contours; this study) projected on the same fault striking 155° and dipping 47°. The red and blue stars are the two main shocks hypocentral locations. The black line is the intersection of the N210° segment and the N155° fault.

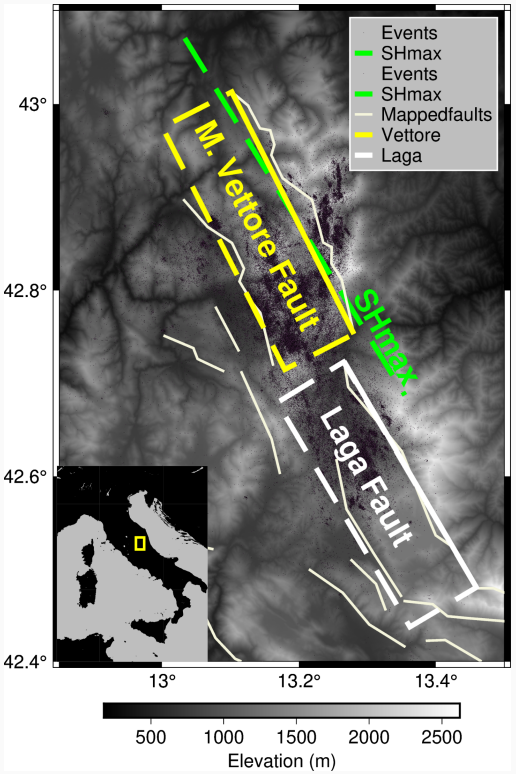

Modified by O. Scotti from Scognamiglio et al. (2018)

Seismic Hazard in Central Italy

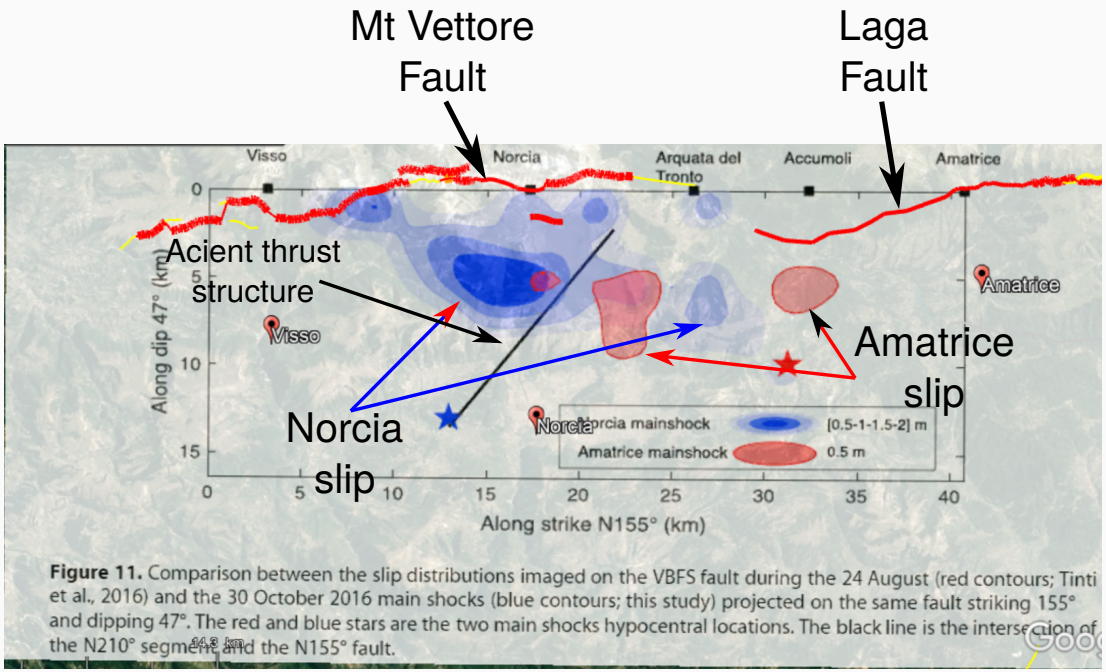

Figure 11. Comparison between the slip distributions imaged on the VBFS fault during the 24 August (red contours; Tinti et al., 2016) and the 30 October 2016 main shocks (blue contours; this study) projected on the same fault striking 155° and dipping 47°. The red and blue stars are the two main shocks hypocentral locations. The black line is the intersection of the N210° segment and the N155° fault.

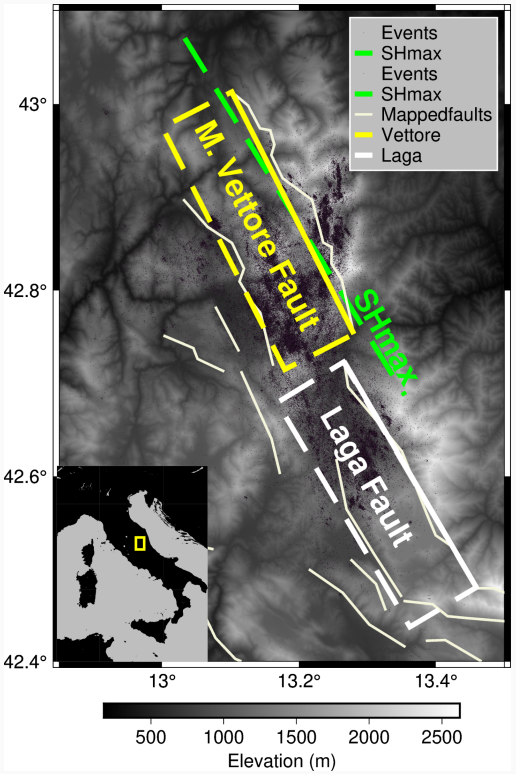

Modified by O. Scotti from Scognamiglio et al. (2018)

Seismic Hazard in Central Italy

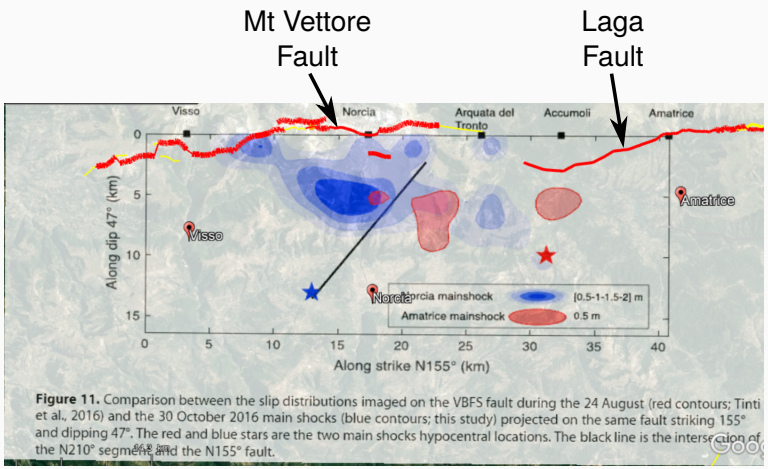

Figure 11. Comparison between the slip distributions imaged on the VBFS fault during the 24 August (red contours; Tinti et al., 2016) and the 30 October 2016 main shocks (blue contours; this study) projected on the same fault striking 155° and dipping 47°. The red and blue stars are the two main shocks hypocentral locations. The black line is the intersection of the N210° segment and the N155° fault.

Rupture jump across step-overs

- Potential larger magnitudes?
- Conditions promoting this?
  - Geometry
  - Stress conditions
- To enhance SHA!

Investigate the physical conditons promoting rupture jumps across step overs regarding normal fault systems

Previous studies focused on strike-slip fault systems: Galis et al. (2015); Hu et al. (2016); Bai and Ampuero (2017); Li and Liu (2020); Oglesby (2008), and more ...

Preliminary exploration

Preliminary exploration: Geometry and settings

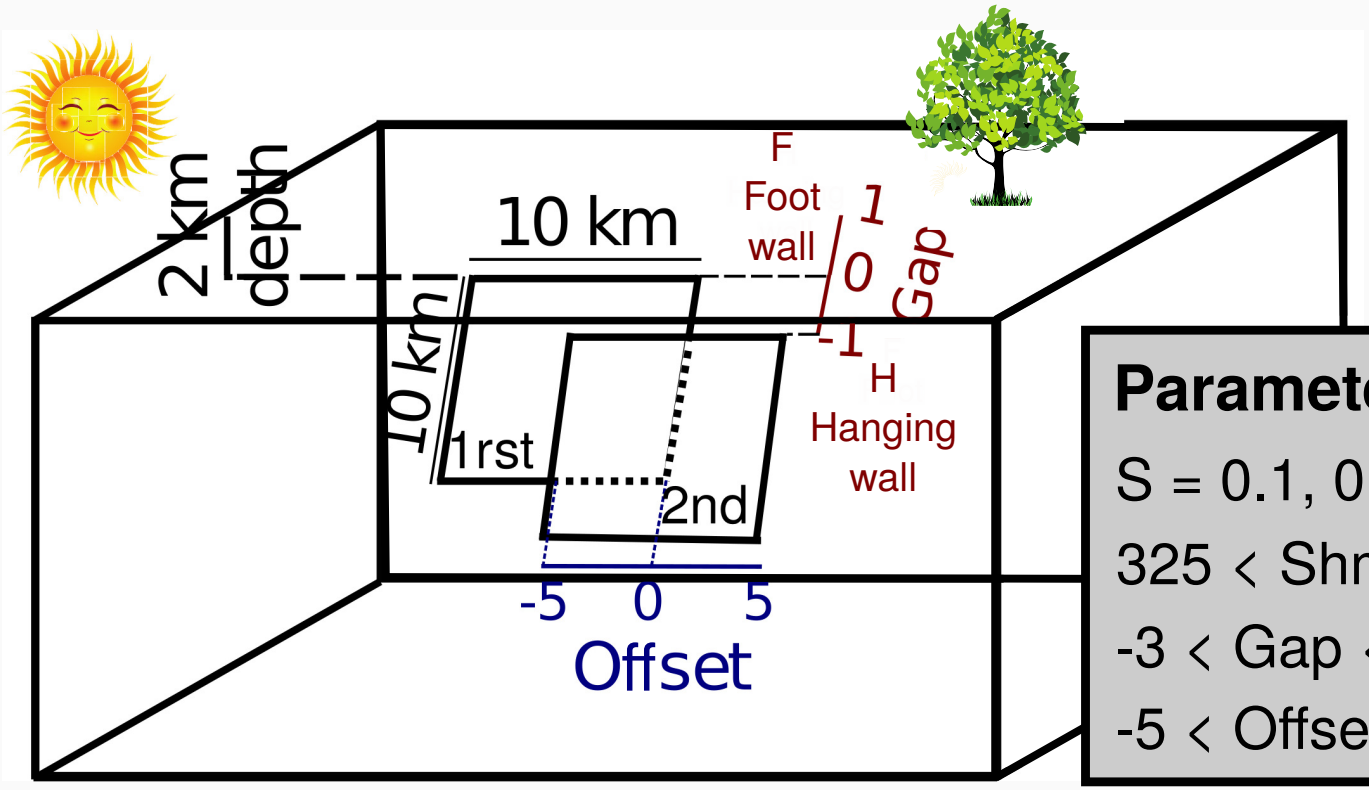

Parameters:

S = 0.1, 0.2, 0.3, ...

325 < Shmax < 350

-3 < Gap < 3 km

-5 < Offset < 5 km

(www.seissol.org; e.g., Wollherr et al., 2018; Ulrich et al., 2019)

SMALL PUBLICITÉ !!

SimModeler: meshing engine

&

SeisSol: dynamic rupture modeling

SimModeler software : Modeling complex fault geometry

ISTerre

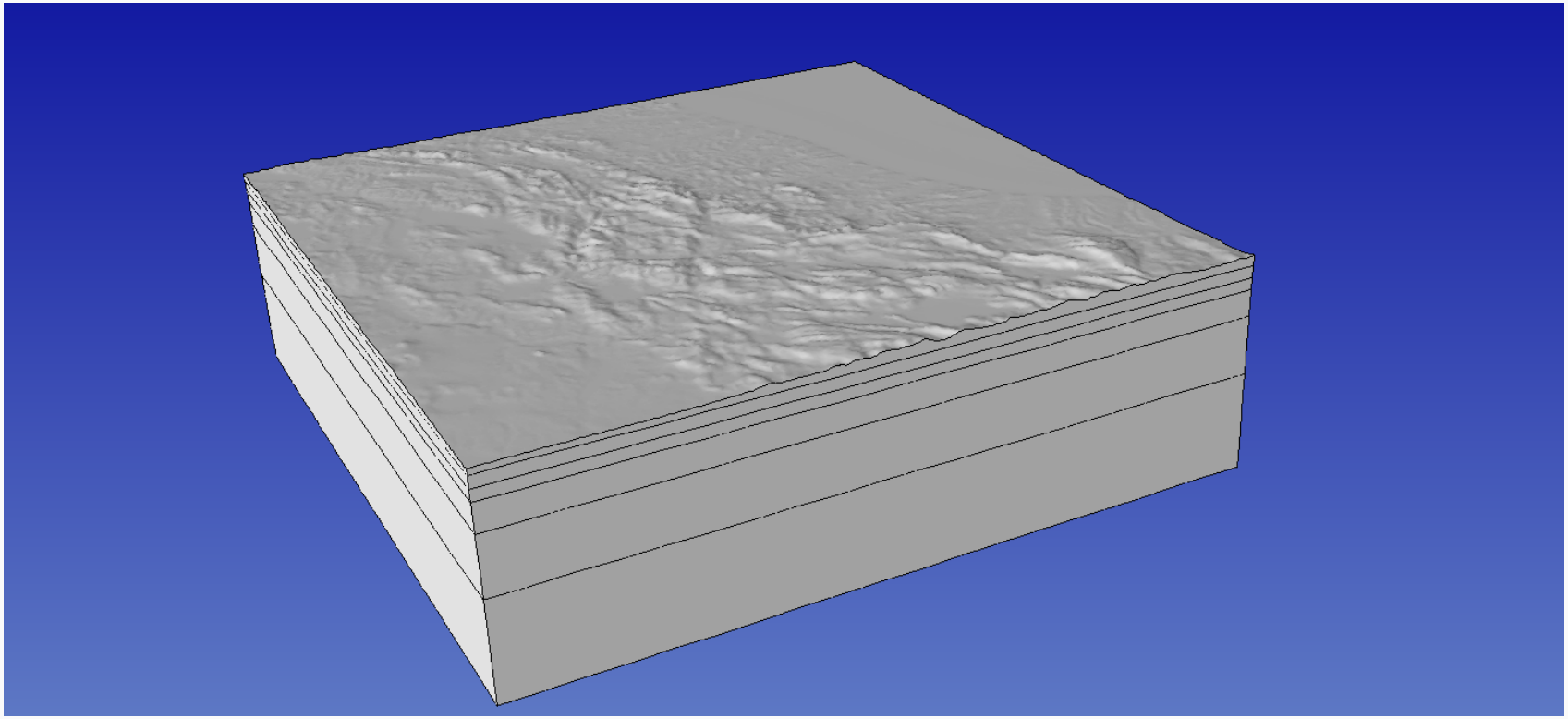

SimModeler software : Modeling complex fault geometry

ISTerre

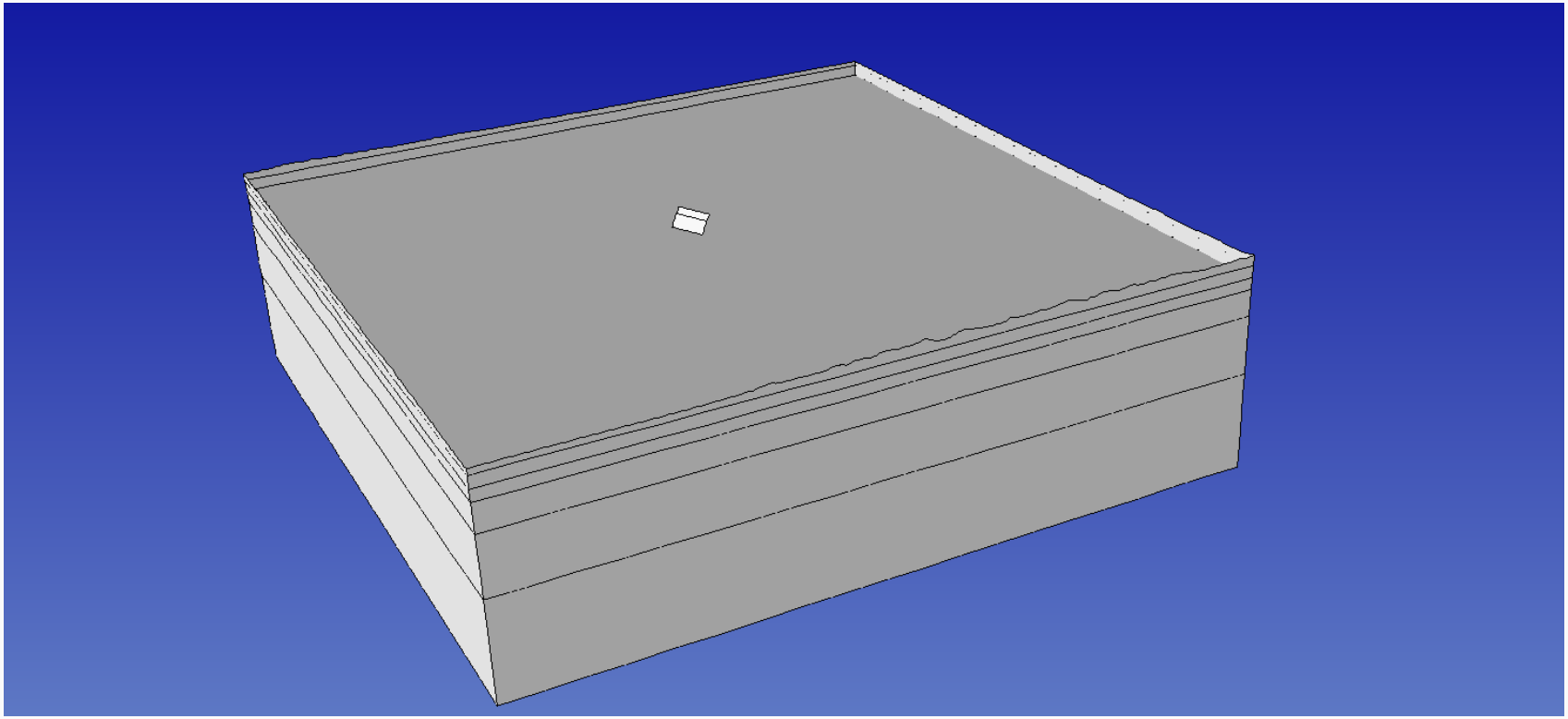

SimModeler software : Modeling complex fault geometry

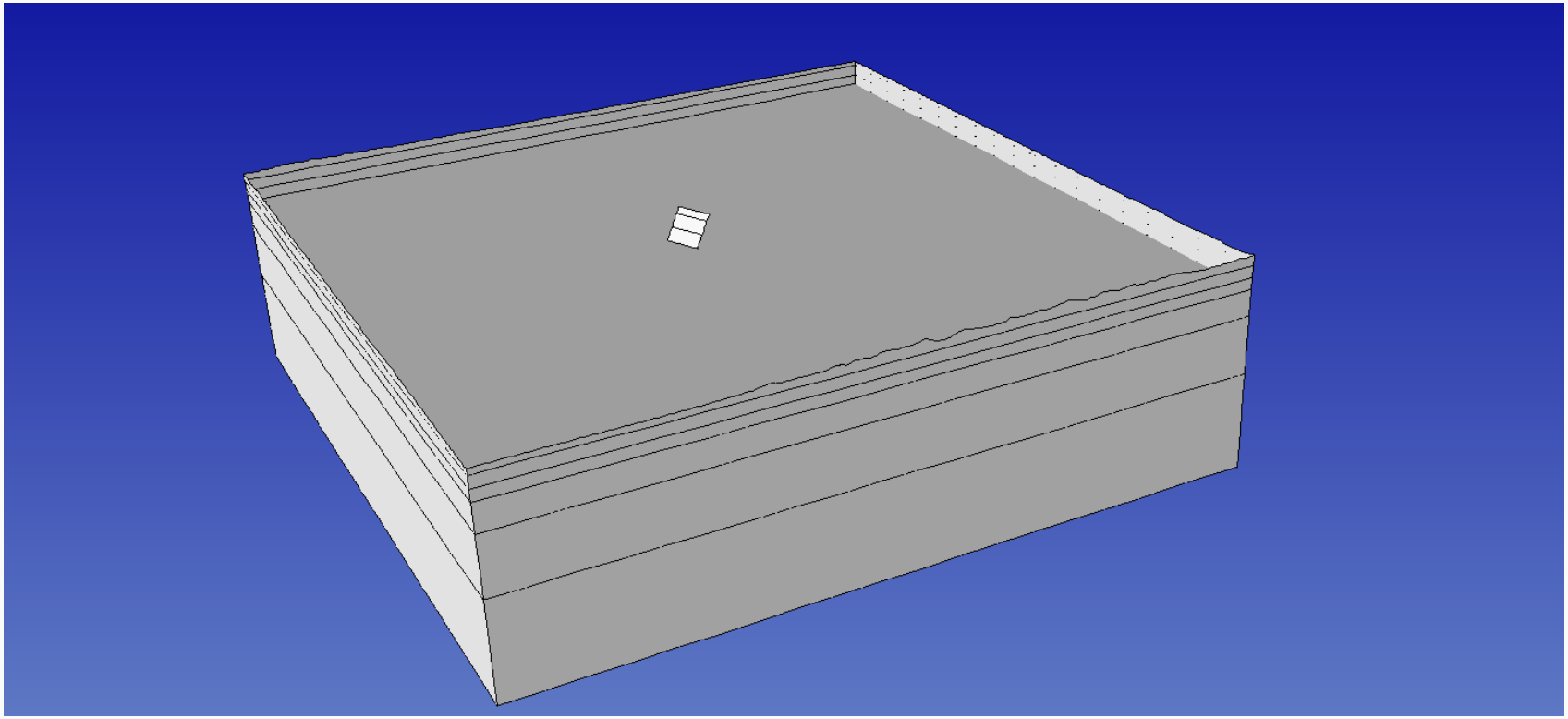

SimModeler software : Modeling complex fault geometry

ISTerre

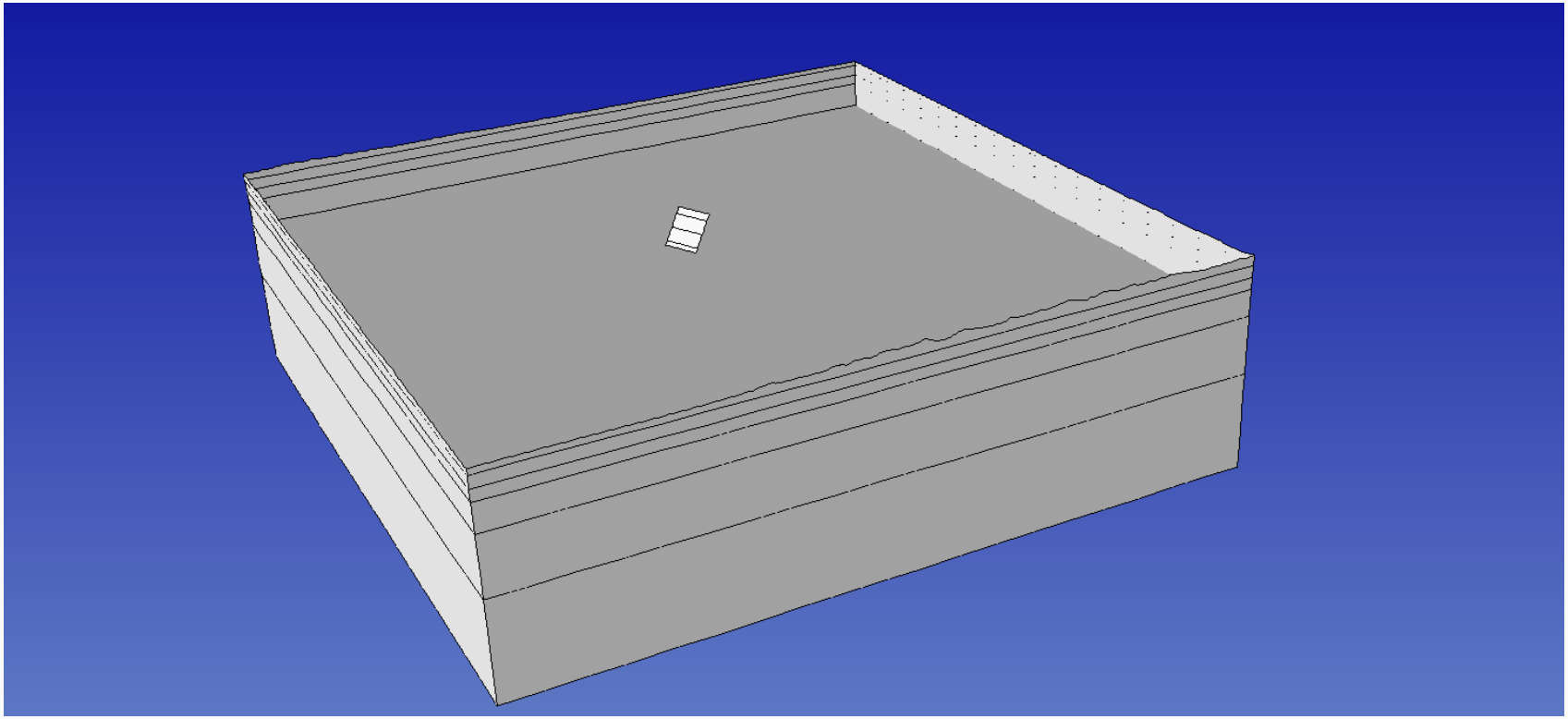

SimModeler software : Modeling complex fault geometry

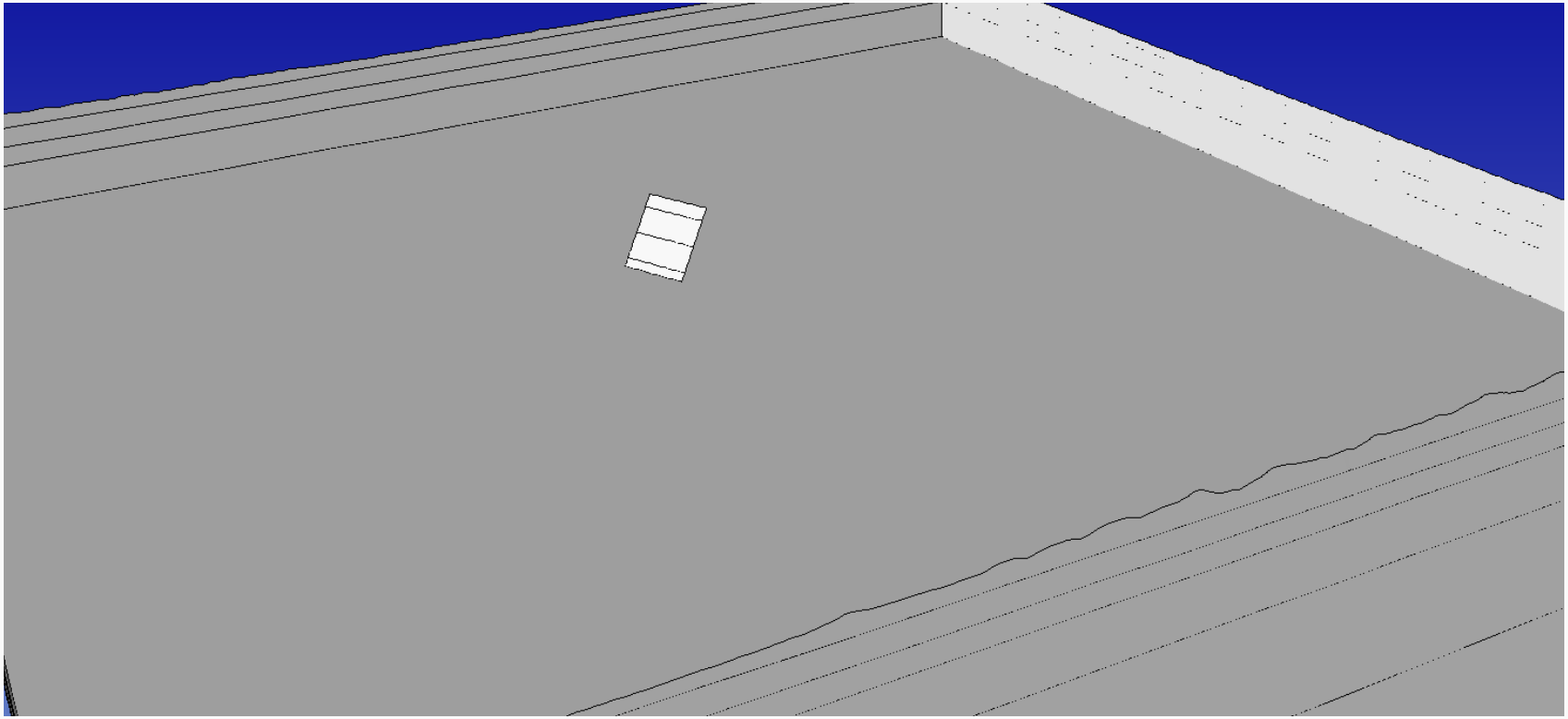

SimModeler software : Modeling complex fault geometry

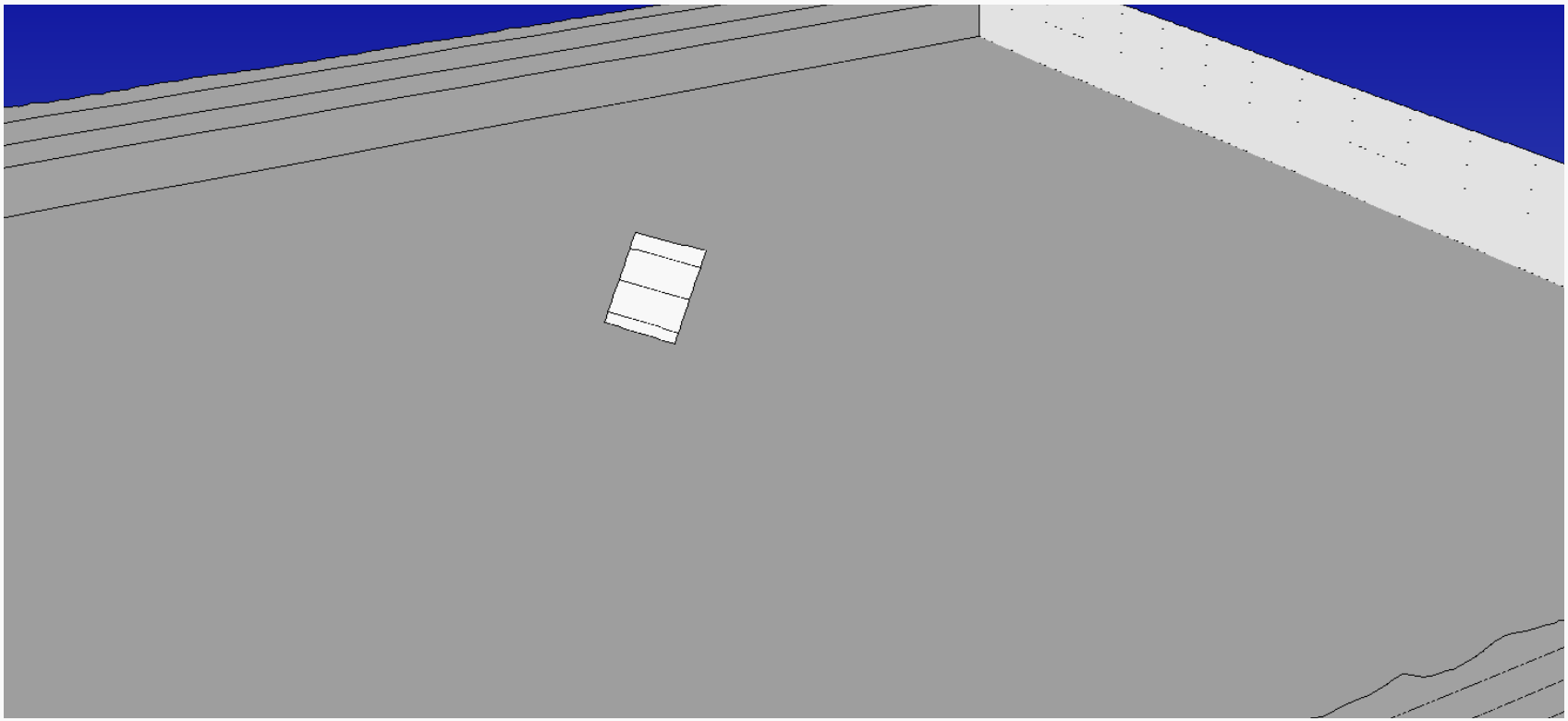

SimModeler software : Modeling complex fault geometry

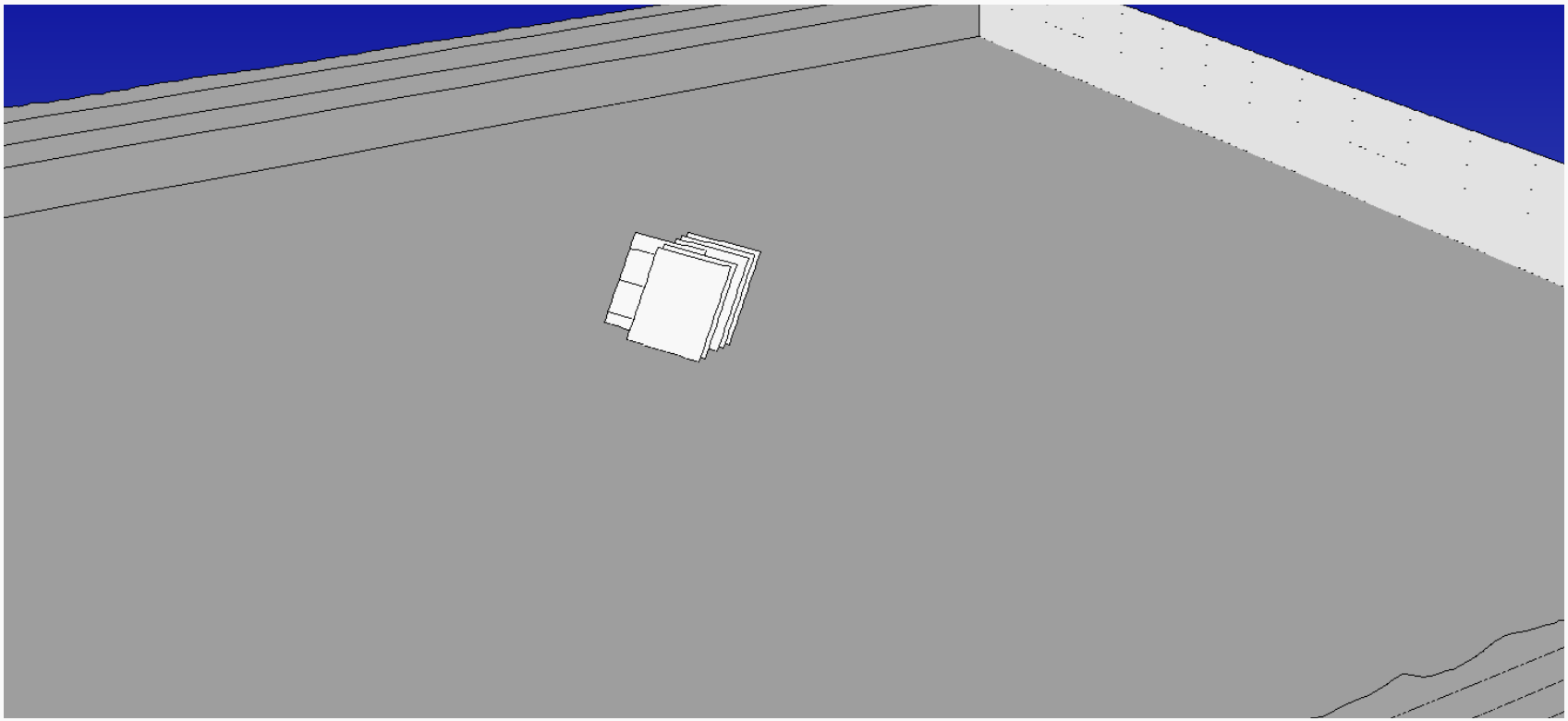

SimModeler software : Modeling complex fault geometry

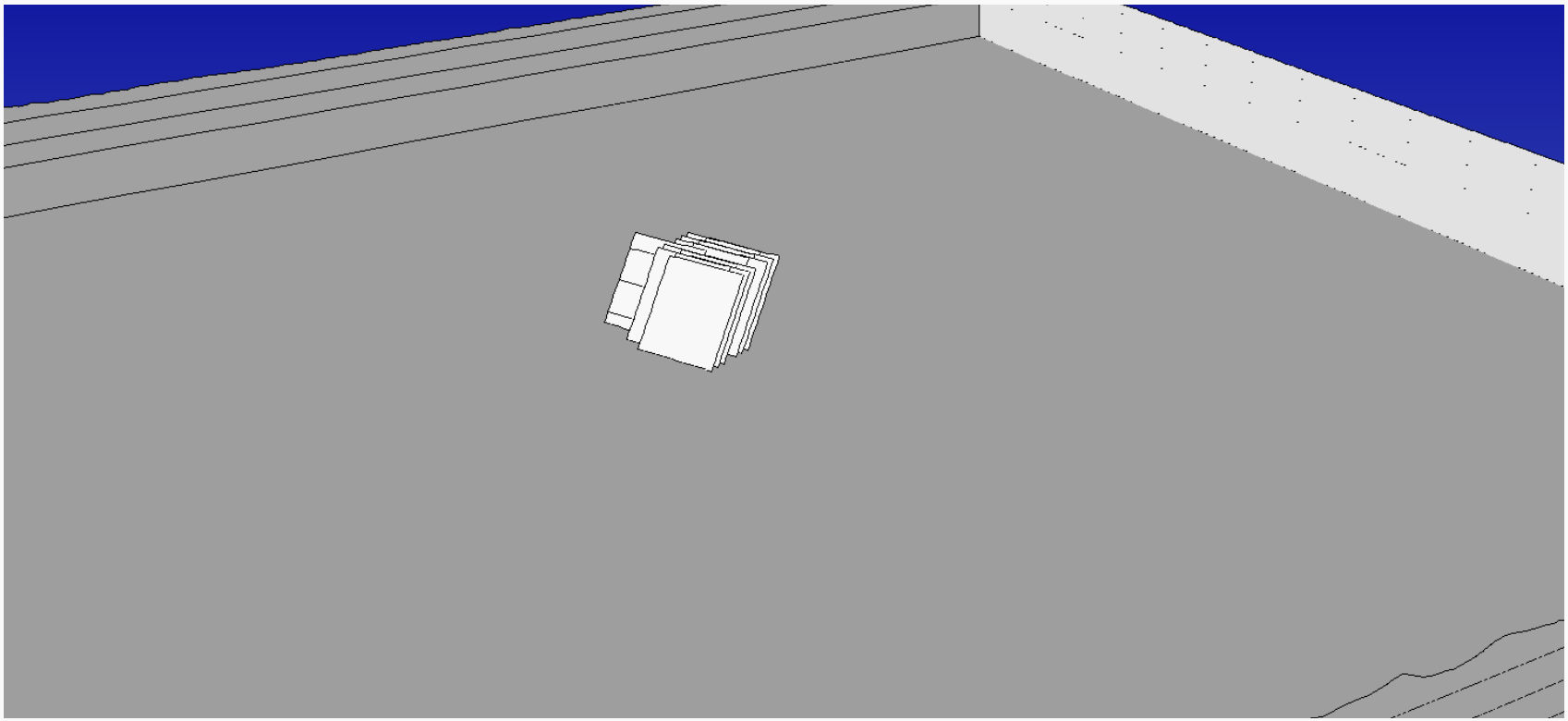

SimModeler software : Modeling complex fault geometry

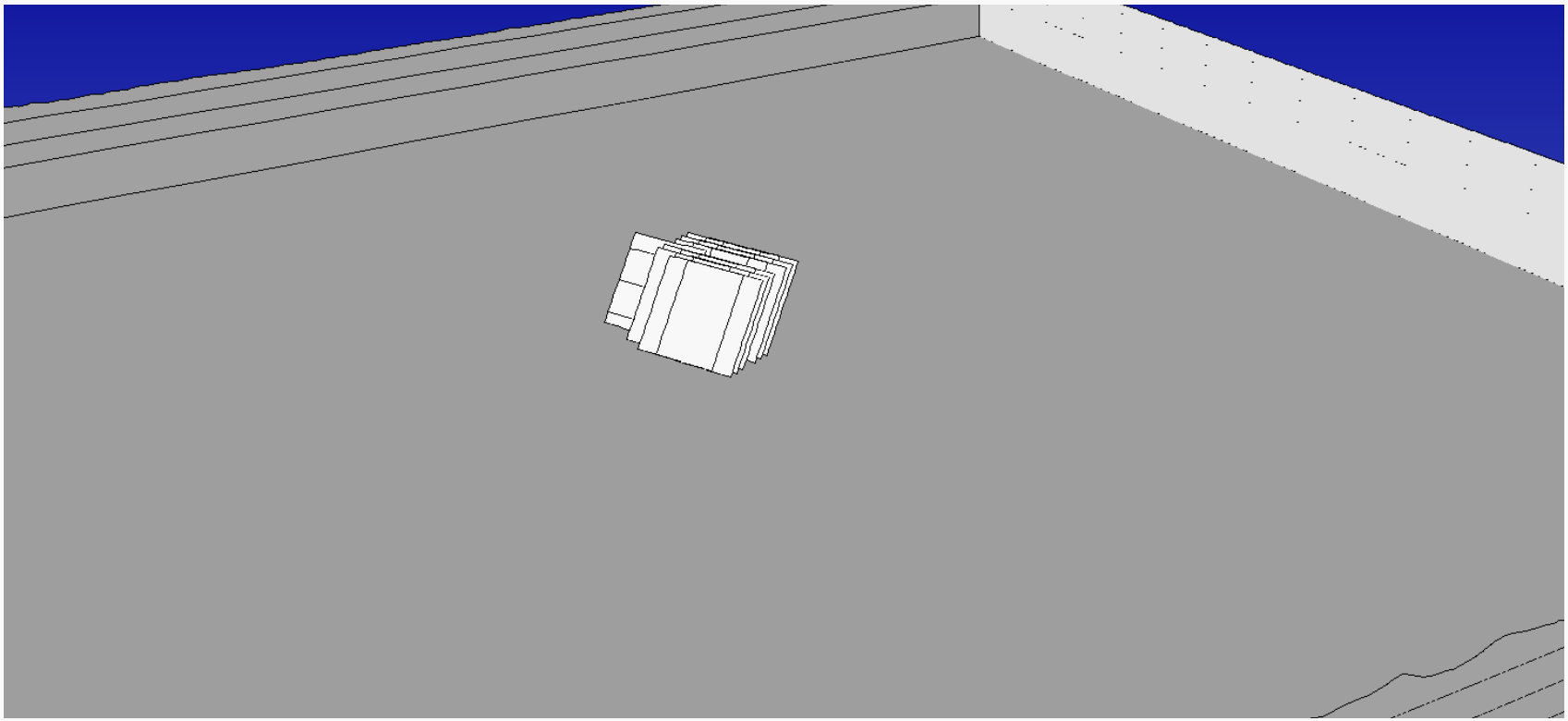

SimModeler software : Modeling complex fault geometry

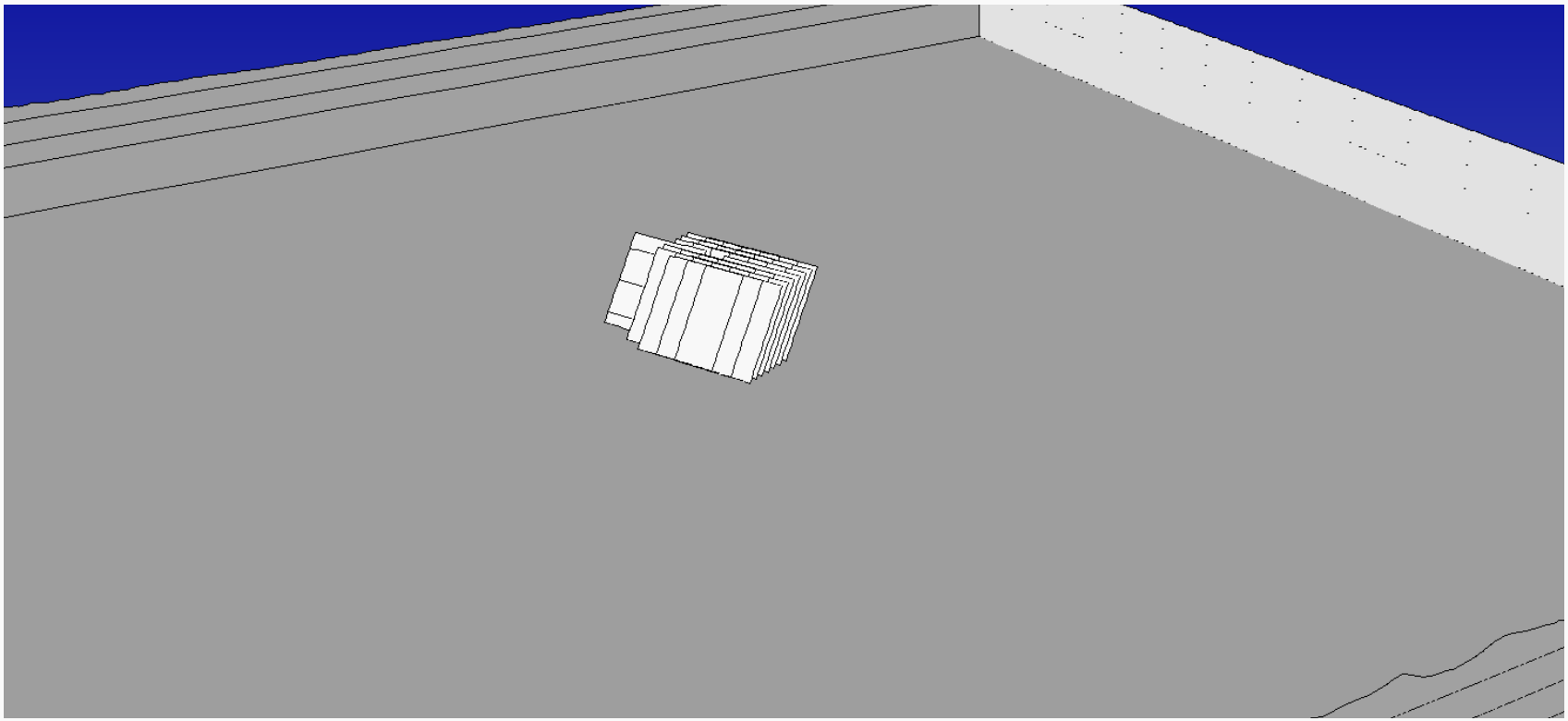

SimModeler software : Modeling complex fault geometry

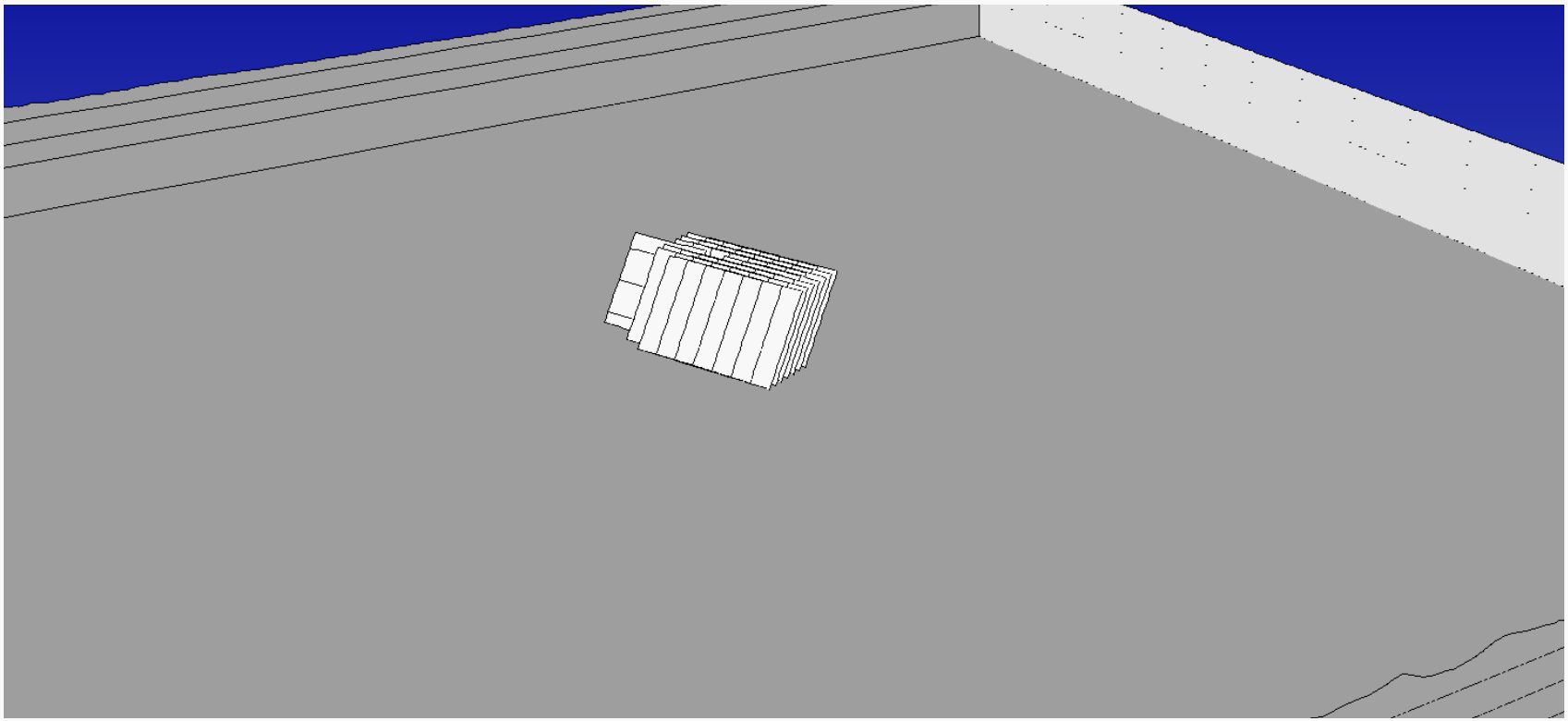

SimModeler software : Modeling complex fault geometry

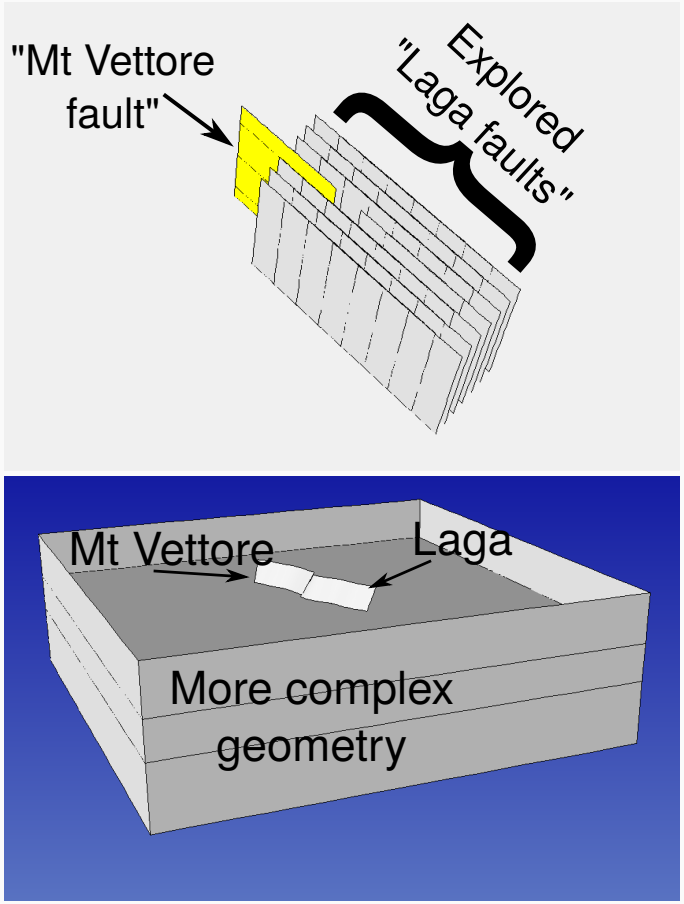

SimModeler & SimModSuite

- Complex mesh & fault geometries

SimModeler software : Modeling complex fault geometry

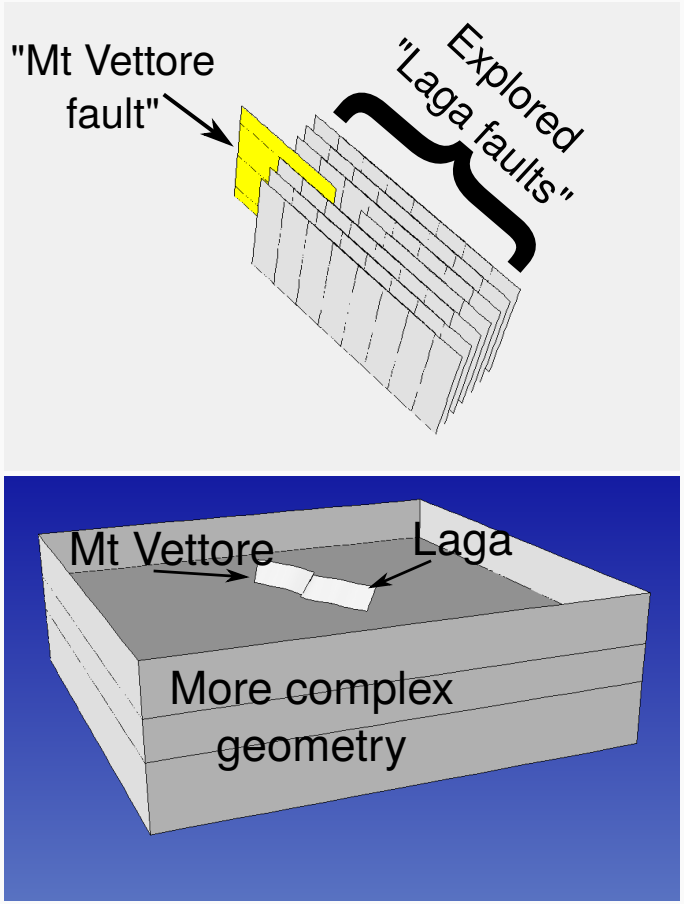

SimModeler & SimModSuite

- Complex mesh & fault geometries
- Mesh adaptivity

SimModeler software : Modeling complex fault geometry

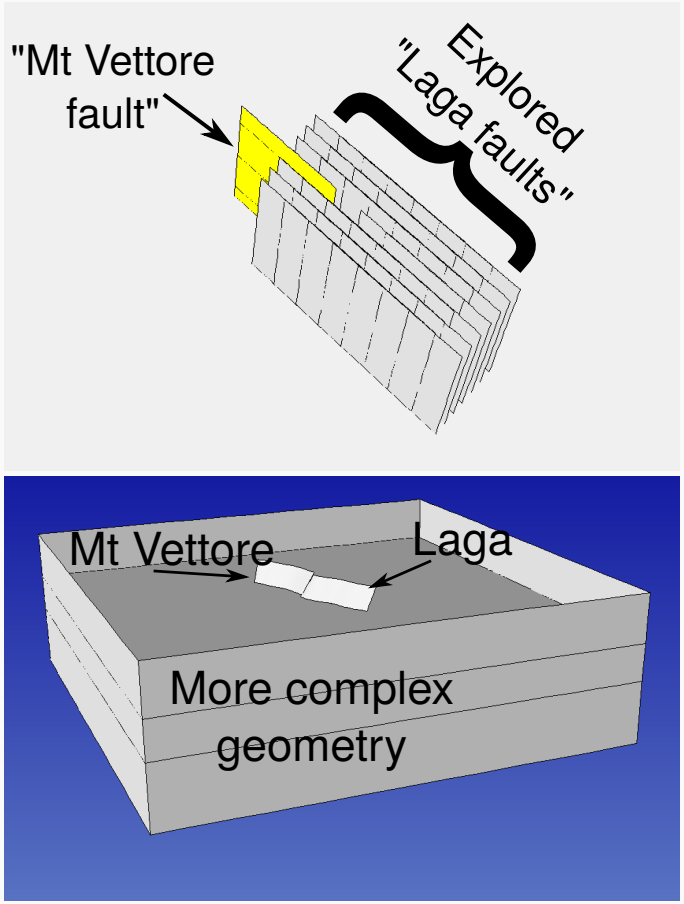

SimModeler & SimModSuite

- Complex mesh & fault geometries
- Mesh adaptivity
- Simple user-friendly interface

SimModeler software : Modeling complex fault geometry

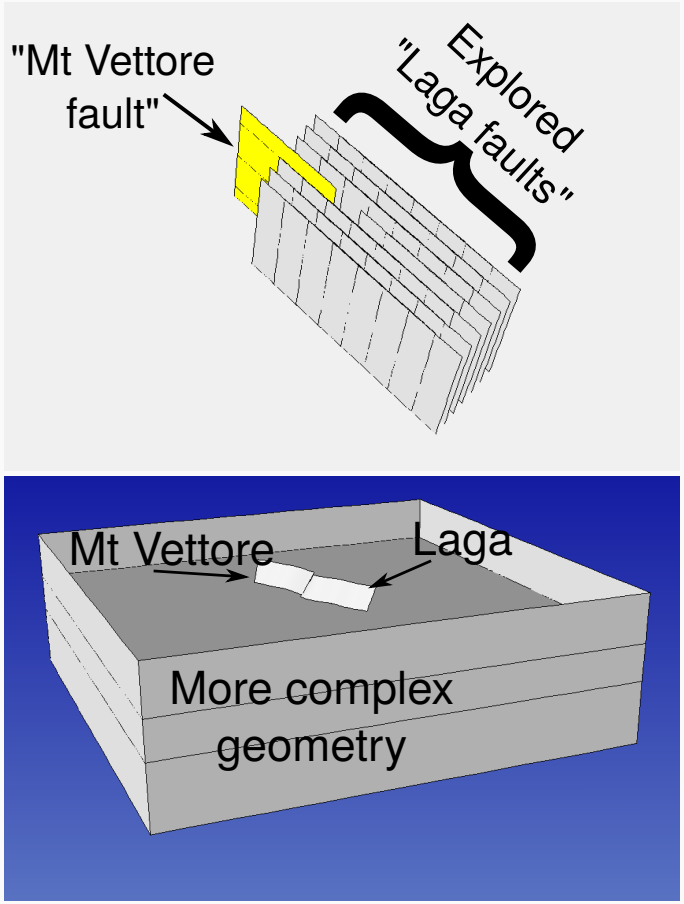

SimModeler & SimModSuite

- Complex mesh & fault geometries
- Mesh adaptivity
- Simple user-friendly interface
- Academic **Free** License

SimModeler software : Modeling complex fault geometry

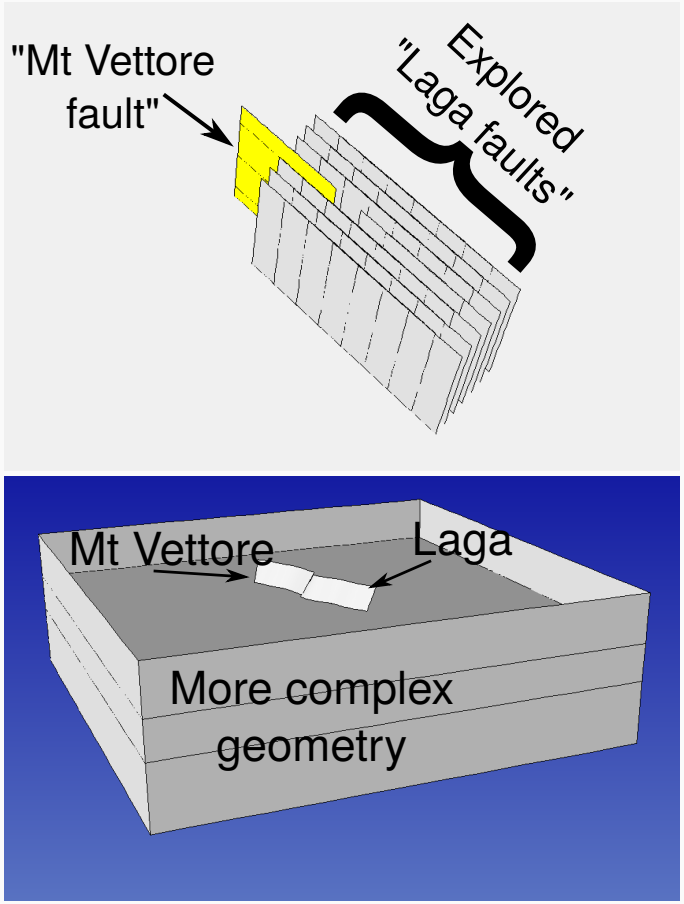

SimModeler & SimModSuite

- Complex mesh & fault geometries
- Mesh adaptivity
- Simple user-friendly interface
- Academic **Free** License
- Available documentation

SimModeler software : Modeling complex fault geometry

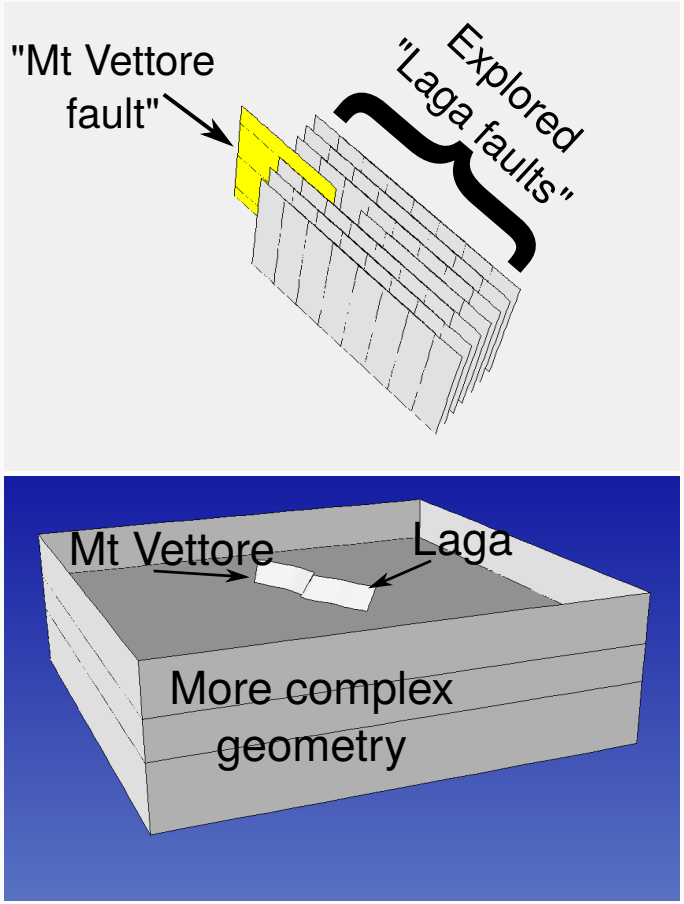

SimModeler & SimModSuite

- Complex mesh & fault geometries
- Mesh adaptivity
- Simple user-friendly interface
- Academic **Free** License
- Available documentation
- Currently being installed on IST-OAR ... Thanks Jean-Noel!

Preliminary exploration: Stress conditions

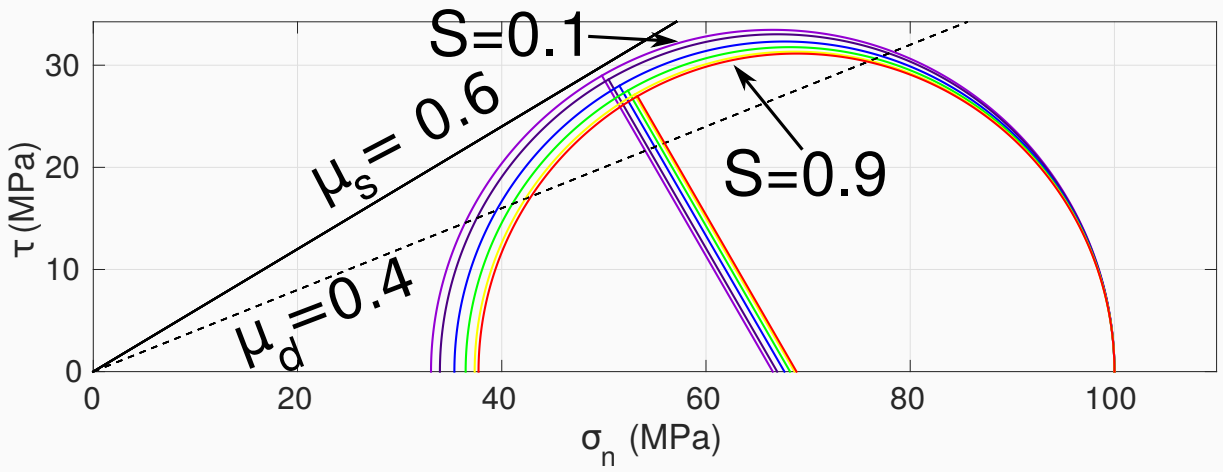

Stress-Strength dimensionless ratio

$$S = \frac{\tau_p - \tau_0}{\tau_0 - \tau_r}$$

Stress & medium conditions

- Stress levels explored

  $S = 0.1, 0.2, 0.4, 0.6, 0.8, 0.9$

Preliminary exploration: Stress conditions

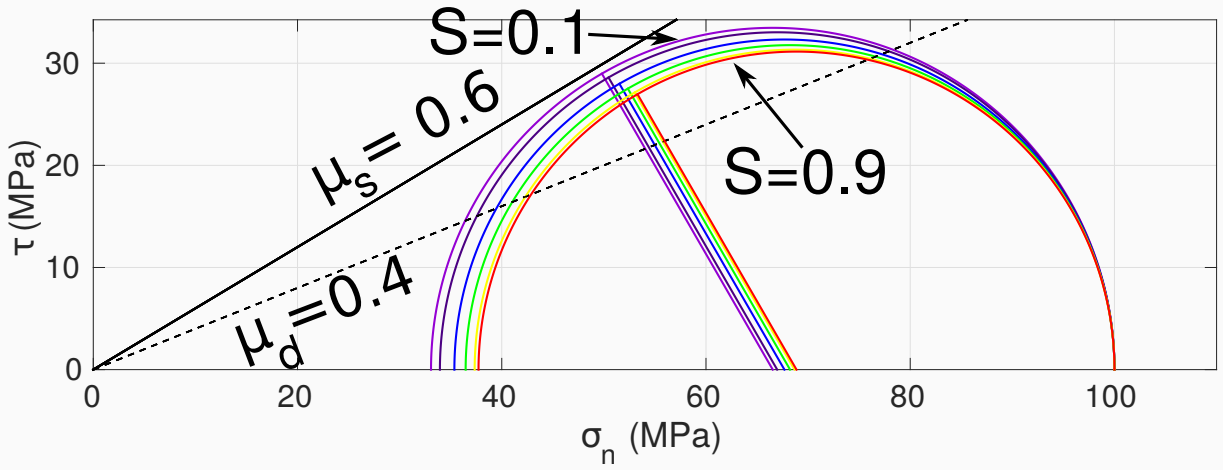

Stress-Strength dimensionless ratio

$$S = \frac{\tau_p - \tau_0}{\tau_0 - \tau_r}$$

Stress & medium conditions

- Stress levels explored
  $S = 0.1, 0.2, 0.4, 0.6, 0.8, 0.9$
- Linear Slip Weakening:
  μ_s=0.6, μ_d=0.4, d_c=0.15 m

Preliminary exploration: Stress conditions

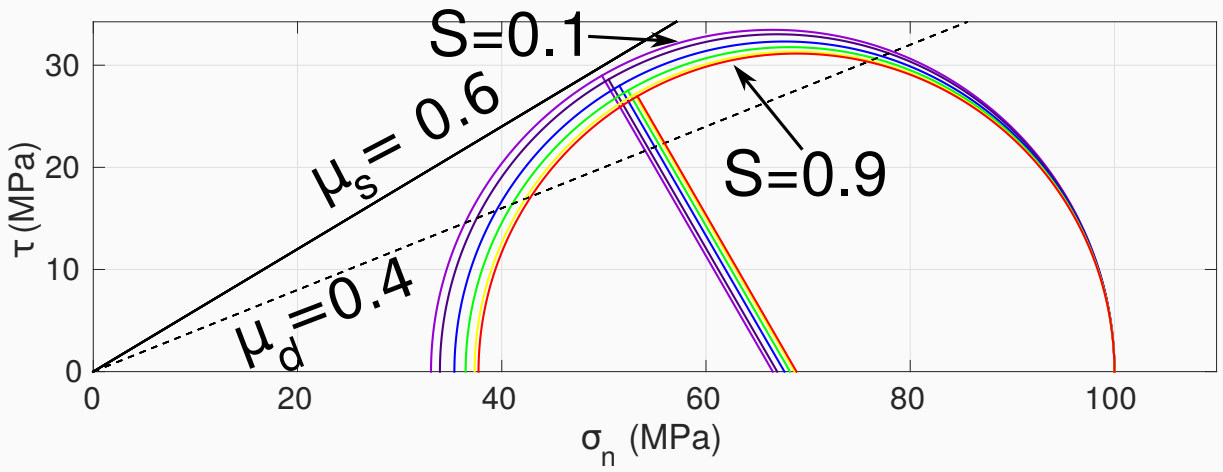

Stress-Strength dimensionless ratio

$$S = \frac{\tau_p - \tau_0}{\tau_0 - \tau_r}$$

Stress & medium conditions

- Stress levels explored
  $S = 0.1, 0.2, 0.4, 0.6, 0.8, 0.9$
- Linear Slip Weakening:
  μ_s=0.6, μ_d=0.4, d_c=0.15 m
- Slow rupture initiation

  $$\mu_s \xrightarrow[t \to 1]{} \mu_d$$

  at a 4×4 km^2 patch

Preliminary exploration: Stress conditions

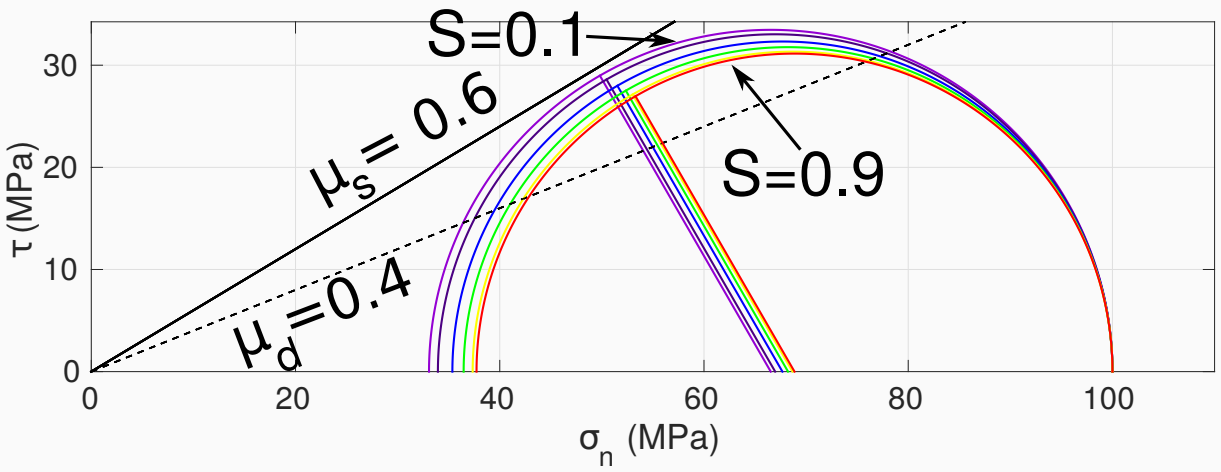

Stress-Strength dimensionless ratio

$$S = \frac{\tau_p - \tau_0}{\tau_0 - \tau_r}$$

Stress & medium conditions

- Stress levels explored
  S = 0.1, 0.2, 0.4, 0.6, 0.8, 0.9
- Linear Slip Weakening:
  μ_s=0.6, μ_d=0.4, d_c=0.15 m
- Slow rupture initiation
  $$\mu_s \xrightarrow[t \to 1]{} \mu_d$$
  at a 4×4 km^2 patch

- σ_{zz} depth-dependent
  $\sigma_{zz} = (\rho - 1x10^3) * g * \min(-1.5x10^3, z)$

Preliminary exploration: Stress conditions

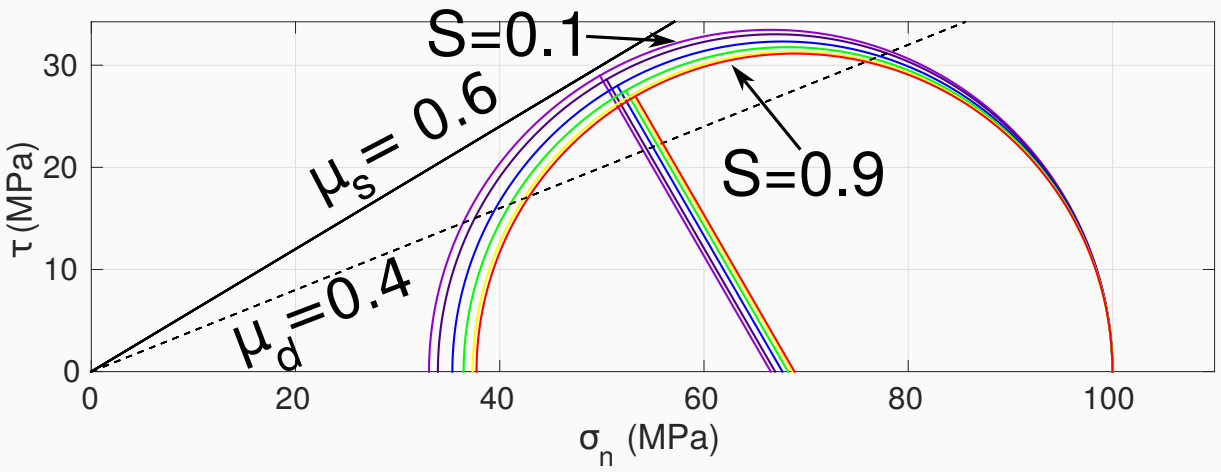

Stress-Strength dimensionless ratio

$$S = \frac{\tau_p - \tau_0}{\tau_0 - \tau_r}$$

Stress & medium conditions

- Stress levels explored
  S = 0.1, 0.2, 0.4, 0.6, 0.8, 0.9
- Linear Slip Weakening:
  μ_s=0.6, μ_d=0.4, d_c=0.15 m
- Slow rupture initiation
  $$\mu_s \xrightarrow[t \to 1]{} \mu_d$$
  at a 4×4 km^2 patch
- σ_{zz} depth-dependent
  $\sigma_{zz} = (\rho - 1x10^3) * g * \min(-1.5x10^3, z)$
- Layered medium from Tinti et al. (2021)

Preliminary exploration: Stress conditions

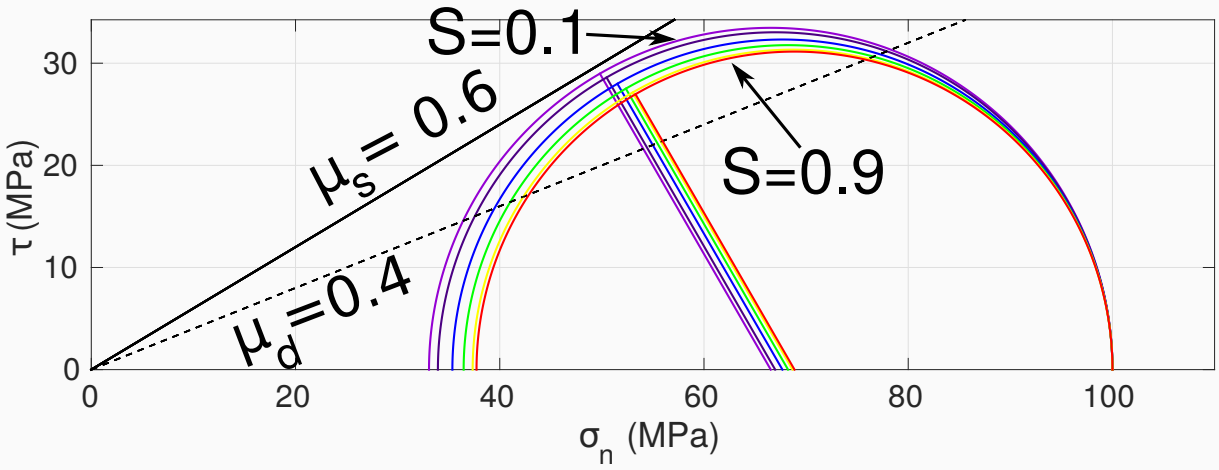

Stress-Strength dimensionless ratio

$$S = \frac{\tau_p - \tau_0}{\tau_0 - \tau_r}$$

Stress & medium conditions

- Stress levels explored
  S = 0.1, 0.2, 0.4, 0.6, 0.8, 0.9
- Linear Slip Weakening:
  μ_s=0.6, μ_d=0.4, d_c=0.15 m
- Slow rupture initiation
  $$\mu_s \xrightarrow[t \to 1]{} \mu_d$$
  at a 4×4 km^2 patch
- σ_{zz} depth-dependent
  $\sigma_{zz} = (\rho - 1x10^3) * g * \min(-1.5x10^3, z)$
- Layered medium from Tinti et al. (2021)
- Faults share same stress level

Inspired by Aochi (2018)

References

References

Aochi, H. (2018). Dynamic asymmetry of normal and reverse faults due to constrained depth-dependent stress accumulation. *Geophysical Journal International*, 215(3):2134–2143.

Bai, K. and Ampuero, J.-P. (2017). Effect of seismogenic depth and background stress on physical limits of earthquake rupture across fault step overs. *Journal of Geophysical Research: Solid Earth*, 122(12):10–280.

Galis, M., Pelties, C., Kristek, J., Moczo, P., Ampuero, J.-P., and Mai, P. M. (2015). On the initiation of sustained slip-weakening ruptures by localized stresses. *Geophysical Journal International*, 200(2):890–909.

Hu, F., Zhang, Z., and Chen, X. (2016). Investigation of earthquake jump distance for strike-slip step overs based on 3-d dynamic rupture simulations in an elastic half-space. *Journal of Geophysical Research: Solid Earth*, 121(2):994–1006.

Li, G. and Liu, Y. (2020). Earthquake rupture through a step-over fault system: An exploratory numerical study of the leech river fault, southern vancouver island. *Journal of Geophysical Research: Solid Earth*, 125(11):e2020JB020059.

Oglesby, D. (2008). Rupture termination and jump on parallel offset faults. *Bulletin of the Seismological Society of America*, 98(1):440–447.

Scognamiglio, L., Tinti, E., Casarotti, E., Pucci, S., Villani, F., Cocco, M., Magnoni, F., Michelini, A., and Dreger, D. (2018). Complex fault geometry and rupture dynamics of the mw 6.5, 30 october 2016, central italy earthquake. *Journal of Geophysical Research: Solid Earth*, 123(4):2943–2964.

Ulrich, T., Vater, S., Madden, E. H., Behrens, J., van Dinther, Y., Van Zelst, I., Fielding, E. J., Liang, C., and Gabriel, A.-A. (2019). Coupled, physics-based modeling reveals earthquake displacements are critical to the 2018 palu, sulawesi tsunami. *Pure and Applied Geophysics*, 176(10):4069–4109.

Wollherr, S., Gabriel, A.-A., and Uphoff, C. (2018). Off-fault plasticity in three-dimensional dynamic rupture simulations using a modal discontinuous galerkin method on unstructured meshes: implementation, verification and application. *Geophysical Journal International*, 214(3):1556–1584.